NEW SUBSTANCES, MATERIALS, AND COATINGS

Electrolytic Plasma Processing for Plating Coatings and Treating Metals and Alloys

A. D. Pogrebnyak[a], A. Sh. Kaverina[a], and M. K. Kylyshkanov[b]

[a] *Sumy State University, ul. Rymskogo-Korsakova 2, Sumy, 40007 Ukraine*
[b] *Serikbayev East Kazakhstan State Technical University, ul. A.K. Protozanova 69, Ust-Kamenogorsk, 070004 Kazakhstan*
e-mail: alexp@i.ua, mixifox@mail.ru
Received August 2, 2012

Abstract—A review of the methods of electrochemical treatment classified as plasma electrolysis is given. Special attention is paid to the physicochemical processes that proceed in electrolytes and the techniques of surface modification and application of protective coatings. The results of investigation of such coatings and surfaces upon electrolytic plasma processing illustrate the efficiency and effectiveness of the method. Being an efficient technique of the surface treatment, which involves both the surface cleaning and plating the coating, the plasma-electrolytic method is being rapidly developed and adapted for commercial use at present.

DOI: 10.1134/S2070205114010092

INTRODUCTION

The discharge phenomenon caused by electrolysis was discovered more than a century ago [1]. Later, it was studied in detail in the 1930s [2]. However, for the first time it was used in practice as late as in the 1960s when spark discharge was used for applying cadmium niobate on a cadmium anode from a Nb-containing bath [3, 4]. In the 1970s, Markov at al. developed a method of applying an oxide on an aluminum anode under arcing conditions [5, 6]. In a decade, the technique was improved and named microarc oxidation (which seems not exactly accurate) [7]. In the 1980s, possibilities provided by the use of surface discharges for plating oxides on various metals were considered in detail by the groups of Gordienko [8, 9], Markov [10], and Kurze [11—13]. The first attempts to use the method in industry were made at that time [14, 15]. Research groups in the United States and China also started investigations in the field [16, 17]. Because of the fragmentary information about the phenomenology of the processes, the terminology adopted by the aforementioned groups was different. As a result, essentially the same method has been referred to as microplasma oxidation, anodic-spark electrolysis, plasma-electrolytic anodic treatment, and anodic oxidation at spark discharges. These are typical examples of the definition of the general concept of plasma-electrolytic oxidation (PEO).

In this work, in order to clarify the basic principles of the aforementioned plasma-electrolytic processes, we use a general denomination, namely electrolytic plasma technology (EPT), which covers a number of methods (oxidation, deposition, saturation, etc.) [18—52].

Electrolytic plasma processing of metals is a promising modern method of production of the components and parts of engines and instruments. Its value and importance are determined by the possibility to use it instead of a number of conventional processes, which either cannot provide a sufficiently high quality of the treatment (surface cleaning, sputtering, diffusion saturation, etc.) or are related to harmful conditions of production and pollution of environment (etching and removal of surface layers of a material)[52—76].

With the use of EPT, different procedures can be carried out, namely, changes in the surface layers—in particular, their hardness, surface adhesion of coatings, and resistance in an aggressive environment or at high temperature. The processes involve nitriding, carbonization, silicification, borating, etc. [76—98].

The advantages of EPT are favorable characteristics of gas discharges, such as low persistence and the possibility of varying parameters in broad ranges [86—101].

Electrolytic plasma technology enables one to obtain coatings with either crystalline or amorphous structure and a broad spectrum of functionality on aluminum, magnesium, titanium, and zirconium alloy surfaces. Thickness of the coatings can vary from several microns to several tenths of a millimeter. The coatings are characterized by a number of peculiar properties. They can be decorative, hygienic, wear- and corrosion-resistant, electrical and thermal insulating, nonstick, etc. An important aspect is ecological safety of the coatings.

Materials produced by EPT and items made of them are widely used in medicine, household appliances, automobile construction, and engineering.

TECHNIQUE
OF ELECTROLYTIC PROCESSES

Plasma phenomena substantially differ from the basic processes taking place on electrodes due to intensification of both physical and chemical processes [18–20] (Fig. 1).

The processes are used in different fields of applied electrolysis, namely, in plasma heat treatment, melting, welding, cleaning, etching, and polishing, as well as in plating coatings (plasma-electrolytic deposition, PED) [21–23]. PED involves a number of processes, namely, plasma-electrolytic oxidation [21] and plasma-electrolytic saturation (PES), including plasma-electrolytic carbonization (PEC) [24], etc. The method is very promising due to the effectiveness in the formation of surface layers with high tribological characteristics [25–27], as well as corrosion and thermal resistance [18, 28–31]. Surface layers are formed as a result of the modified electrode processes, which are plasma-intensified chemical reactions and diffusion on the electrode surfaces. In most cases, this is anodic oxidation (PEO) or electrolysis of the solution and reduction of cations (PES). The role of the residual physicochemical processes, which proceed due to the presence of plasma and promote the formation of the surface layer, is not as obvious, but they typically depend on and affect the chemical reactions and diffusion and, hence, should be considered as well [32].

Plasma-electrolytic oxidation is treatment at a potential that is higher than the breakdown value of the oxide film that grows on the anodically passivated metal surface. The technique is characterized by the coexistence of several arcs that rapidly move over the treated surface. Plasma thermochemical interactions in numerous surface discharges result in the growth of the coating in both directions from the substrate surface. Although local temperatures are very high, the temperature of the substrate is usually lower than 100°C. Varying concurrently the electrolyte composition and the discharge conditions, one can change the microstructure and phase composition of the substrate in a broad range from metal alloys to complex ceramic oxides [33–37]. As a result, on aluminum-alloy components, one can obtain thick wear-resistant layers (with the maximum hardness of 18 through 23 GPa and the maximum thickness about 500 mm) with a perfect adhesion and a low cost of production.

PES is carried out at a potential higher than the breakdown value of gas bubbles formed on the ingot surface, which can act as either a cathode or an anode with respect to the electrolyte bath. Because of the much higher current density attained at such discharges compared to the usual plasma vacuum treatment, ionic bombardment of the surface can take place and cause the rapid heating and the strong activation of the substrate surface [38–40]. Thus, a short-term treatment (3–5 min) becomes sufficient for the formation of 200- to 500-mm-thick diffusion-satu-

rated layers with good mechanical and corrosion characteristics. The proper selection of electrolyte provides the formation of such compounds as nitrides, carbides, and borides.

PED is carried out in an apparatus that consists of a reservoir filled with electrolyte and a powerful current source. The reservoir is typically made of stainless steel, cooled with water, and serves as a counter-electrode. Conditions of plasma electrolysis can be provided by different current sources [41]. In direct current sources, a double-wave detection scheme is typically used and enables one to set either galvanostatic or potentiostatic current conditions. Pulsed current sources make it possible to interrupt the process repeatedly and, hence, control the arc duration [42–44]. However, pulsed current can cause an additional polarization of the electrode surface due to the creation of a charged double layer. In this case, the higher voltages (up to 1000 V) can be necessary for providing the necessary current density. Pulsed constant-current conditions are widely used in PES techniques where a relatively low voltage (typically lower than 450 V) is sufficient. For example, a silicon-controlled rectifier with a power of 10 kW, which provides direct current in a voltage range of 0 through 450 V, is used for carbonization and nitriding under plasma electrolysis conditions. High power and/or a set of different frequencies can be provided by heteropolar pulsed current sources.

Owing to their simplicity, PED processes successfully compete in cost with the vacuum application of coatings and galvanic techniques [45–53]. The preliminary treatment of coatings involves cleaning and degreasing. No additional procedure, such as annealing or surface activation, is needed.

For application of coatings, specimens are connected to a current source and usually immersed in a bath to a depth of 30–50 mm under the electrolyte surface. The main parameter that should be controlled during the PEO treatment is the current density. Usually, plasma electrolysis is carried out at a current density of 0.01–0.3 A/cm². According to the first Faraday law, the current density determines the growth rate of the coating. In the course of coating growth, the voltage increases, at first rapidly, then slowly, and finally reaches a constant value of plasma existence. The critical rate of the voltage change corresponds to spark discharge on the electrode surface U_s. The value strongly depends on the characteristics of a particular metal–electrolyte system and falls in a range of 120–350 V.

By contrast to the oxidation, the main parameter that should be controlled during the PES process is voltage. The temperature should be constant both at the first stage, when the voltage rapidly increases, and at the second stage when the voltage is constant. In both cases, upon the formation of the coating, the specimens are only rinsed with water and dried.

PEO treatment requires a thorough selection of metal–electrolyte systems [54, 55]. The most reason-
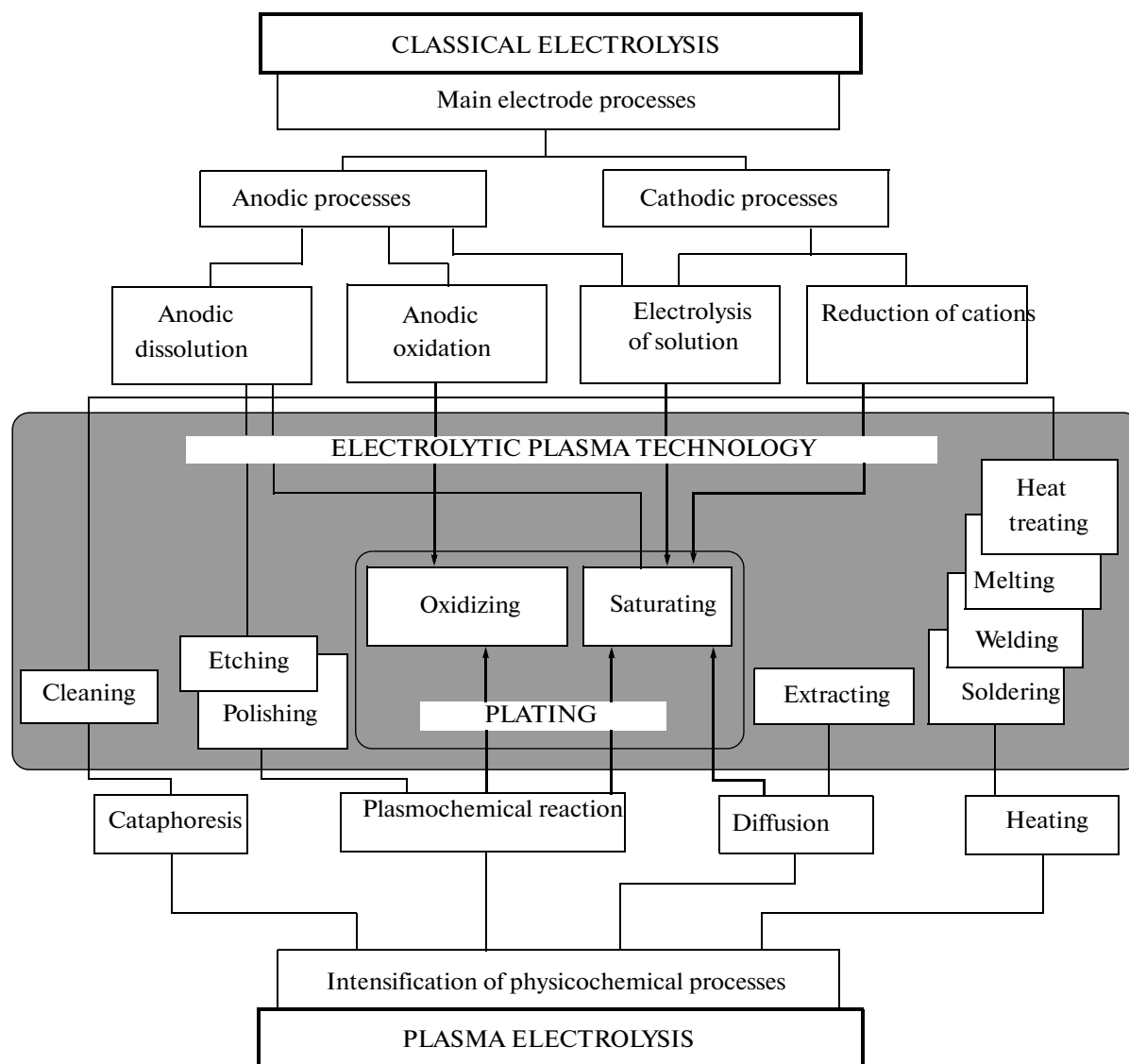
Fig. 1. A scheme of physicochemical processes typical of plasma electrolysis and main conventional electrode reactions that proceed during electrolytic plasma treatment [98].

able electrolytes are fluorides with complex behavior (NaF, KF), electrolytes that provide weak passivation of the metal, and those in which metal passivation is strong, e.g., boric acids and salts of carbonic and phosphoric acids, inorganic polymers (silicate, aluminate, wolframite, and molybdenite), and alkaline metal phosphates, which can form polymer anions. In these electrolytes, spark-discharge voltages can easily be achieved. With respect to the contribution to the composition of coatings, electrolytes can be divided into the following groups:

(i) solutions that supply oxygen solely to the coating;

(ii) electrolytes that contain anionic components and contribute some other elements to the coating;

(iii) electrolytes that contain cationic components and contribute some other elements; and

(iv) suspensions that provide cataphoretic transport of macroparticles, which are included in the coating.

In electrolytes of the second and third groups, coatings are formed both due to the oxidation of substrate and the inclusion of electrolyte components in the surface layer. As a result, a broad spectrum of surface compositions with various properties can be produced. Therefore, such bases are considered as the most promising. Colloidal solutions of sodium or potassium silicate, as well as multicomponent silicate-based electrolytes, are widely used for PEO treatment.

In addition to silicate, the bath can contain substances that increase the conductivity of the electrolyte, e.g., Na (0.5 to 2.0 g/L), NaOH or KOH (1 to 50 g/L), provide the formation of an oxide layer, which involves stabilizing components, e.g., $Na_2B_4O_7 \cdot$

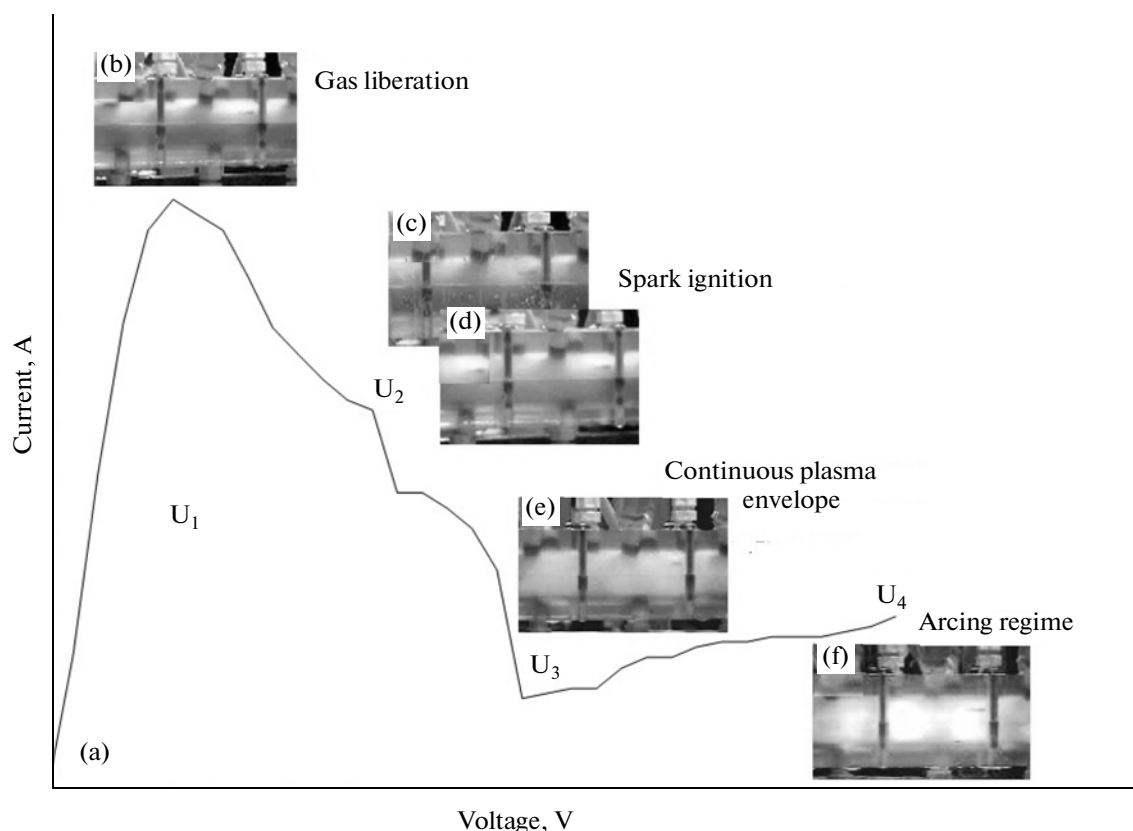**Fig. 2.** Voltammetric curve of the plasma-electrolytic process under cathodic conditions [41].

$10H_2O$ (40 g/L), glycerin (10 g/L), Na_2CO_3 or K_2CO_3 (≤ 500 g/L), and modifying components, e.g., $NaAlO_2$ (2–20 g/L) or $Na_6P_6O_{18}$ (≤ 150 g/L). For some particular purposes, in order to provide cataphoretic effects during oxidation, fine powders of solid materials with high melting points and/or dry paste (for improving the wear and friction resistance) can be added to the bath. Thus, depending on the electrolyte composition and the electrode polarity, one can use PEO and PES techniques profitably.

PROCESSES OF PLASMA-ELECTROLYTIC TREATMENT

Figure 2 shows results of treatment of a wire (AISI 1080, high-carbon steel) in a dynamic system where electrolyte was supplied at a velocity of 3–5 L/min and the wire was moved through the EPT chamber (reactor) at a velocity of 3 m/min. The voltammetric curve reflects different stages of the process.

At low voltages U_1, the current increases in proportion to the voltage in conformity with the Faraday law. Under these conditions, a gas, typically H_2, is liberated, as shown in Fig. 2b. When the voltage is further increased, the U_2 point (>90 V), which is interesting in view of the electrocatalytic plasma processes, is reached. This range is characterized by the appearance of glowing gas, which is unstable, as indicated by the

substantial variations in the current values. The current shown in Fig. 2 under these conditions is the mean value of the actually oscillating current. Figures 2c and 2d illustrate the instability, which is accompanied by spark ignition of the gas. The appearance of glowing gas was determined by evaporation of electrolyte close to the electrode (in this case, cathode) due to the Joule heat. Experimental studies [56] carried out neglecting the Joule heat showed that normal electrolysis is impossible without the formation of a glowing gas, because there is no electrolytic gas liberation that would increase with an increase in the voltage.

The color of the glow depends on the nature of metals involved in the alloy composition. For example, orange plasma was observed in the presence of sodium ions, while blue plasma is seen with zinc ions. The colors are determined by the plasma discharge on the working surface of the specimen when different elements emit light waves of certain lengths.

When the voltage is increased to the U_3 value, the cathode is continuously enveloped in gas plasma, which is characterized by a substantial decrease in the current values. These EPT conditions correspond to the stable plasma when one can carry out a controlled surface treatment (Fig. 2e). The conditions were discovered by Kellogg and are called Kellogg's range.
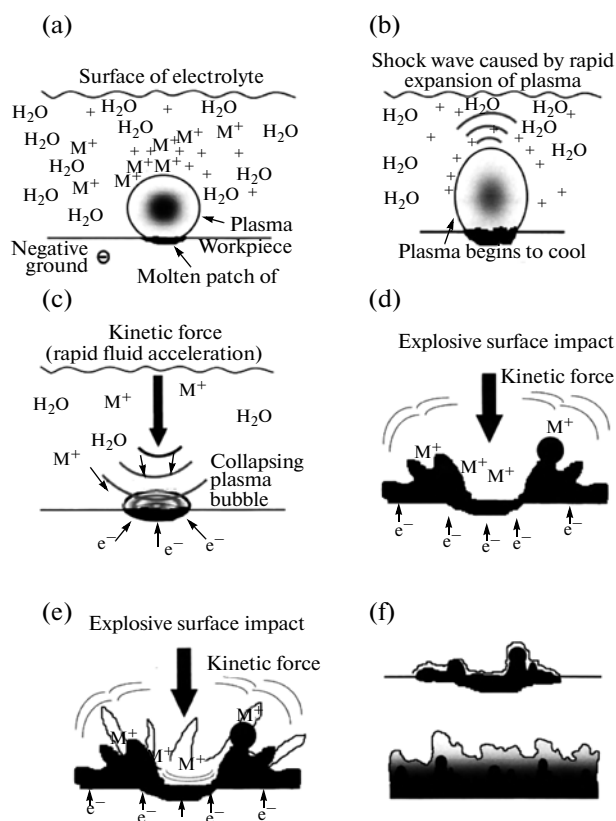
(a)   (b)

Surface of electrolyte   Shock wave caused by rapid
                                                     expansion of plasma

Negative ground

Plasma

Workpiece

Molten patch of

Plasma begins to cool

(c)   (d)

Kinetic force
(rapid fluid acceleration)   Explosive surface impact

Kinetic force

Collapsing
plasma
bubble

(e)   (f)

Explosive surface impact

Kinetic force

Fig. 3. A scheme of successive stages of electrolytic plasma treatment [41].

The critical current density under conditions of the appearance of stable plasma is known to depend on a number of factors, including the shape (planar or round), size and orientation of electrode. As was shown in experimental studies, when the diameter of an anode wire increases, the formation of stable plasma takes place at the higher voltage and current density. The result agrees with the data obtained in independent studies of the cathodic conditions. When the voltage is increased to U_4 value, both intensive sparking and a plasma envelope around the electrode are observed (Fig. 2f). These aggressive conditions can produce a baneful effect on the surface of a specimen [54, 55].

As can be seen in Fig. 3, under stable plasma conditions, the ingot is enveloped in a gas shell. The high potential difference between the electrodes results in the accumulation of positive ions, which are always present in the electrolyte, in close vicinity to the cathode, chiefly on the surfaces of gas bubbles. Thus, a very high positive charge is located very close to the cathode. As a result, the high electric-field intensity is strongly localized between the cathode and the zone of positive charge. During the plasma-electrolytic oxidation, the electric-field intensity of the plasma layer can be as high as 105 V/m or higher [57−61]. When such an electric-field intensity is reached, the gas inside

bubbles is ionized and a plasma discharge appears. Figure 3a shows a magnified image of such working surface. Only one plasma bubble is shown for clarity. In a real system, the number of bubbles is very large. At some points inside plasma, the temperature can be as high as 2000°C. Hot bubbles are surrounded with a relatively cool electrolyte (about 100°C), which causes the cooling of plasma. As a result, bubbles are burst on a metal surface (Figs. 3b−3g). The duration of plasma discharge is about 10^{-6} s. The whole surface of the cathode is not covered with a continuous plasma layer; at each time moment, the surface is covered with a certain number of discrete plasma discharges.

When a bubble is burst, two phenomena can occur:

(i) positive ions, which were arranged around the bubble, are accumulated directly on the cathode surface; and

(ii) the accumulated energy is released in the gas layer, and the kinetic energy is transferred to the liquid layer and then to the working surface of the specimen; the energy can be very high and the ions originally accelerated by the explosion of the burst bubble continue to move toward the electrode surface due to the kinetic energy, which results in the deposition of metal ions contained in the electrolyte on the working surface of the specimen (Figs. 3e, 3f).

Composition of electrolyte for plasma-electrolytic saturation [98]

Process	Purpose	Bath composition
Nitriding	Increase in surface hardness, wear and corrosion resistance, and fatigue strength	$NaNO_3$, 45%
Carbonization	Increase in surface hardness, wear resistance, and fatigue strength	$C_3H_5(OH)_3$, 15%; Na_2CO_3, 5%
Binding	Increase in surface, heat, and wear resistance	$Na_2B_4O_7$, 3%; $NaOH$, 45%
Carbonization + nitriding	Increase in surface hardness and wear resistance	$C_3H_5(OH)_3$, 15%; Na_2NO_2, 45%
Carbonization + saturation with boron	Increase in surface hardness and wear resistance	$Na_2B_4O_7$, 3%; $NaNO_2$, 45%
Nitriding + saturation with boron	Increase in surface hardness and corrosion resistance	$C_3H_5(OH)_3$, 15%; $Na_2B_4O_7$, 3% $NaNO_2$, 45%

During plasma-electrolytic treatment, the motion of ions is determined chiefly by their acceleration through the plasma and their consumption at the bubble burst. EPT is a dynamic system where the electrolyte flow at a high velocity through the reactor chamber results in rapid transfer of ions to the plasma layer. Hydrodynamic flow, combined with efficient ionic transport during the deposition in the course of EPT, results in a high deposition rate.

DIFFUSION AND PLASMA-CHEMICAL REACTIONS. CATAPHORETIC EFFECTS

The difference in chemical compositions between the heated surface of the metal electrode and a gas cloud is the factor that determines the diffusion in EPT. Both inner diffusion of elements toward the metallic substrate (i.e., saturation) and diffusion toward the surface take place. The surface saturation is possible during both anodic and cathodic processes [62−65]. Depending on the nature of electrolyte, a composite saturation with nonmetals such as O, C, N, and B (and their combinations) or carbide-forming transition metals such as W, Mo, V, etc, is possible. The saturation of anodic surfaces with nonmetal elements is usually carried out in aqueous solutions of simple inorganic salts containing the necessary elements and certain organic compounds (table).

The diffusing substances are selected in such a way that they can be negatively ionized in the electrolyte, transferred to the gas cloud under the effect of the applied electric field, and accelerated by the voltage drop to bombard the electrode surface. The restricted content of the diffusing elements on the electrode surface is determined by their concentration in the neighboring gas cloud. Therefore, the formation of compounds on the anode is also often accompanied by oxidation and the oxide layer is often present on the surfaces of, e.g., carbide, nitride, or boride layers. In order to eliminate surface oxidation, one can use the cathodic polarization technique [42−44].

Diffusion of metals into the electrode surface can be provided by the use of interpolar acids. The maximum content of diffusing elements in the electrode is determined by their concentration in the adsorbed polymer layer. In order to increase the concentration of diffusing elements in the layer, one can increase the concentration of the electrolyte and/or take acids with longer polymer chains. The very high diffusion rate reached in this way is a distinguishing advantage of PES. Compared to usual processes of thermally activated saturation, the effective diffusivity at the plasma electrolysis increases by 200−250% in the case of nonmetals and by 30−50% for metals. The following factors seem to cause the above effects:

(i) the decrease in the activation energy of the diffusion in the electric field;

(ii) the surface activation and the improved adsorption of diffusing elements due to the electric discharge effects; and

(iii) the increase in the bulk-diffusion rate due to the discharge effect.

Another peculiarity of EPT is the surface formation of certain structures, such as metastable high-temperature phases, nonequilibrium solid solutions, mixed complex compounds, glassy (amorphous) phases, etc. These substances are formed as a result of plasma thermochemical reactions on the electrode surfaces [66].

According to the dynamics of discharge phenomena, chemical reactions at plasma electrolysis proceed in two stages, namely, ionization and condensation. At the first stage, collision or thermal ionization in the discharge zone takes place. The reactions that proceed here are chiefly dissociation of compounds. The processes rapidly develop and are accompanied by substantial exothermal effects and volume extension. As a result, high temperatures and pressures are reached in a short time period in plasma within the discharge channel. Electric field in the discharge channel separates the polluted particles in plasma. Some of them (e.g., positive ions) are transferred to the electrolyte, while the residual ones (e.g., negative ions) are

involved in the processes on the electrode surface. At the second stage, the temperature rapidly drops and plasma components form substances that are condensed within discharge channels. Insofar as the cooling rate may be as high as 10^8 K/s, one can find peculiar high-temperature phases, supersaturated solutions, and nonequilibrium compounds on the surface at a temperature that is nearly equal to that of the environment. Thus, α- and γ-Al_2O_3, TiO_2, α-SiO_2, δ-Nb_2O_5, $ClNb_2O_6$, Al_2TiO_5, $BaTiO_3$, $NaNbO_3$, $3Al_2O_3 - 2SiO_2$, and other compounds can be formed on the electrode surfaces.

The phase composition is an important factor that determines the actual mechanical or tribological effect of the surface layer [67–69]. Predicting the phase composition of the treated layer is a topical applied task in the field of EPT. It is difficult to determine the accurate composition of the solid solution, especially taking into account the difficulties in estimating complex kinetic parameters that describe all the reactions proceeding in the discharge zone. A more productive approach that enables one to obtain a quantitative characteristic of the phase composition of the layer was proposed in [70] for plasma-electrolytic oxidation of aluminum. Its efficiency is determined by step-by-step thermodynamic calculation of the equilibrium reaction products at the ionization and condensation-discharge stages. Calculations are based on maximization of entropy of a heterophase multicomponent system, which models the discharge channel. With the use of the approach, one can study the effects of discharge parameters on the phase composition, as well as the effects of the channel composition, its geometry, and thermodynamic state (ρ and T). Studying the properties can be useful for selecting and optimizing the conditions of electrolytic plasma technology.

Cataphoretic effects, i.e., the transfer of macroparticles both from and to the electrode surface, can be observed in strong electric fields reached at the plasma electrolysis. The transfer is promoted by hydration and charging of macro particles, as well as hydrodynamic effects caused by the surface heating and convection. The outer transfer can be used for cleaning surfaces and removing coatings and films formed with other methods. Transfer to the surface is also widely used for increasing the efficiency of plating coatings. The sizes of macro particles and the energy density at plasma electrolysis are two main factors that affect cataphoresis (and hence, the surface structure) in the course of the formation of coatings. First of all, the deposition of submacro particles with the use of cataphoresis from colloidal solutions and the deposition of macro particles from suspensions can be considered independently. Colloidal solutions of inorganic polymers, such as silicates, aluminates, polyphosphates, tungstates, molybdenates, etc., as well as powder suspensions of oxides, nitrides, carbides, borides, etc., can be used for the formation of a broad variety of coatings. Second,

the electric conditions of the plasma electrolysis can conditionally be divided into three main groups:

(i) conditions that facilitate sublimation of macroparticles in a discharge around electrode;

(ii) conditions that promote sintering of macroparticles on the electrode surface; and

(iii) conditions that provide complete synthesis of macroparticles within the growing film.

Although the particular current conditions and electric parameters of the process depend on the selected electrolyte–electrode system, the aforementioned detailed classifications enable one to predict possible structures of the deposited coatings, namely, (I) pseudodiffusion, (II) agglomeration, or (III) compact synthesis.

PROPERTIES OF EPT COATINGS

Microstructures

The combination of mechanical, thermal, chemical, and electric methods in electrolytic plasma technology enables one to produce surfaces with peculiar microstructures. The microstructure of an EPT-cleaned steel surface has been thoroughly studied with the use of focused-ion-beam (FIB) and transmission-electron microscopy (TEM) [71, 72]. The surface microstructure was found to involve a layer with a thickness of 150–250 nm and a grain size of 10–20 nm [73]. Later studies of EPT-cleaned steel surfaces with the use of X-ray diffraction (XRD) and TEM showed that the surface microstructure consists of two or three layers. The upper amorphous layer, as well as the lower layers, is composed of nanoscaled grains, which gradually increase in size until the bulk microstructure is attained. The thickness of the nanograin layer was noted to increase with the increase in the duration of EPT.

Figure 4 shows a TEM image of the cross section of an EPT zinc coating. As can be seen in Fig. 4a, the Zn coating is composed of columnar-like clusters with a width of 350–550 nm. TEM images in light and dark modes showed that clusters are composed of nanoscale subcolumns with a length of 20–40 nm and an area of 5–20 nm. The electron-diffraction pattern shown in Fig. 4b indicates that the deposited Zn coating has a hexagonal structure with a small grain size. Thus, the observations show that the Zn coating is characterized by small grain sizes and grows in the form of compact columns.

Nanoscale grains obtained as a result of EPT (either cleaning or deposition of metals) seem to be determined by the rapid cooling of localized molten surface layers. It is worth noting that investigations of certain steels showed that the main part of microstructure and, hence, the mechanical properties of the material treated do not change in the course of EPT [74, 75].
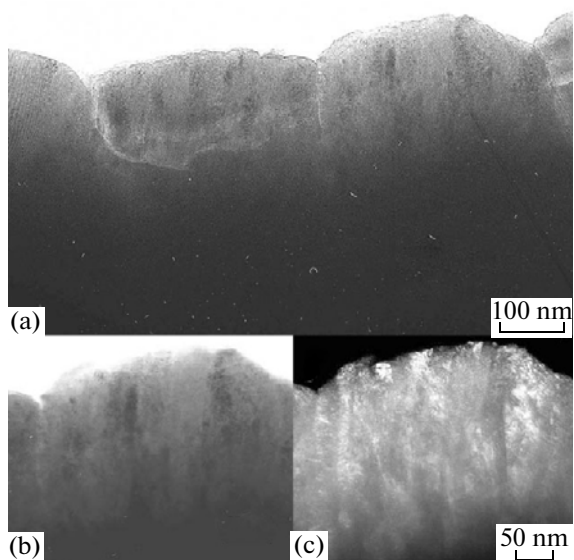
Fig. 4. TEM images of (a) general cross section of a Zn coating at a small magnification and (b) light and (c) dark regions of the section at a large magnification.

Fig. 5. General cross section of a graphite specimen covered with an Al, Al_2O_3 coating.

Plating of Coatings

The role of metallic coatings in the improvement of different surface characteristics, such as corrosion resistance, wear resistance, etc., is very important.

The formation of a protective layer is as follows: the surface of a specimen is covered with an aluminum-based alloy. The layer is applied by gas-thermal spraying with the use of electro-arc sputtering of wires. The technique provides the formation of a sufficiently compact aluminum alloy coating with a porosity of no higher than 4%. Pores in the coating are closed and do not affect the subsequent oxidation. Thickness of oxide coatings on the surfaces of compact materials depends on the electric field intensity and can vary from 5 to 1000 μm [75−77]. In the course of electrolysis, oxygen is liberated at the anode and, being activated by electric discharges, oxidizes the metal. With an increase in the thickness of the oxide layer, the electric field intensity should be increased to stabilize microarc discharges and preserve the electric conditions of the oxidation. The oxidation is attenuating, and to intensify it, one should increase the electric field intensity to a value that provides breakdown of the oxide layer and the formation of arc discharges. The duration of discharges varies in a range of 1×10^{-3} s. Electric discharges at surface sites with the higher local conductivity provide the formation of a compact oxide layer with closed pores.

In the course of the operation of such an item, pores decrease the heat conductivity and act as compensators of voltage drops, which meets the requirement of the protection of items against high-temperature oxidation.
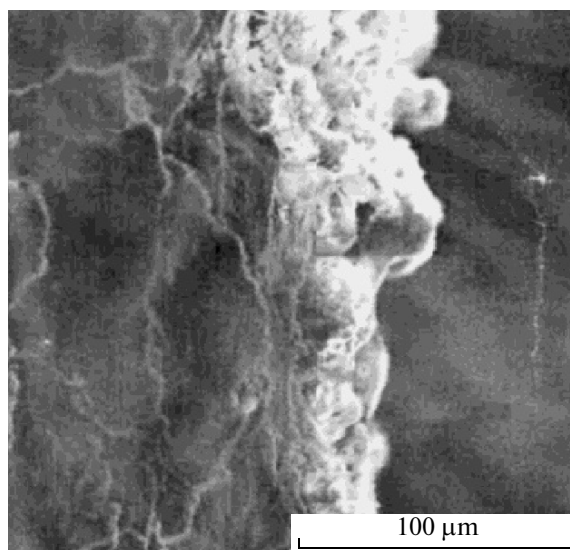
Figure 5 shows the surface of a specimen, which was metalized with aluminum during electrolytic plasma processing with the use of a wire made of technically pure aluminum. Electrodes were made of porous graphite composed of extended grains. Because of the through porosity of the graphite surface and the pore sizes comparable to the sizes of sputtered metal drops, the surface coating was characterized by the inclusion of sputtered material in pores of the graphite substrate. The aluminum layer on the specimen was as thick as 250−350 μm. Arrows show the boundaries of the coating composed of Al_2O_3 and alloying additives and inclusions; the boundary of the Al coating is also shown.

Metal graphic analysis of specimens revealed a higher density of the oxide layer (more than 120 μm) near the aluminum substrate. The surface part of the oxide layer is characterized by high porosity and composed of numerous fritted sites with the shapes of microcraters and droplike traces of oxide-layer fusion. Results of the investigation show that the microarc process is spread within pores of the coating. In the pores, one can also see traces of microarcs localized as fritted craters. The oxide layer is formed not only on the surface of the coating, but also inside pores, as a result of which it has a developed structure within the aluminized layer [77].

Figure 6 shows images of EPT coatings deposited on a stainless steel mount. EPT coatings are compact and follow the substrate structure (Figs. 6c, 6d). As can be seen, EPT can be used for plating coatings on micron-size wires (Fig. 6e), and the coatings are characterized by uniform micro-roughness (Fig. 6f), which provides perfect adhesion to the polymer coat-
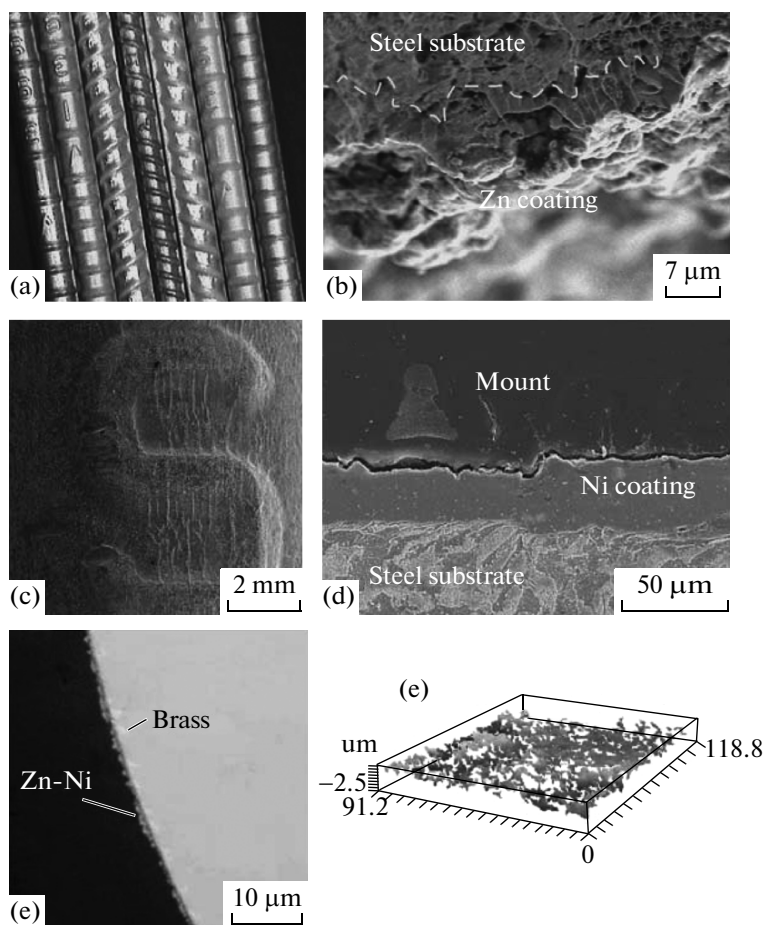
Fig. 6. (a) Metallic and alloyed coatings plated on a mount by plasma electrolysis, (b) fractogram of a Zn coating on a mount upon tensile test (dashed line shows a boundary between the substrate and coating), (c, d) morphology of the surface and cross section of a Ni coating (illustrates the conformity and the absence of defects), and (e, f) cross section and surface profile of a Zn−Ni coating plated on brass covered with metal cord (350 μm in diameter).

ing. Plasma-electrolytic plating of coatings has the following advantages.

(i) High deposition rate (the deposition rate of Zn coatings can be as high as 0.75−1 μm/s).

(ii) Strong interface bonds, namely, perfect adhesion of the coatings to the substrate. As follows from the fractogram of the EPT coating at the single-axis tension (Fig. 6b), the coating does not exfoliate. EPT coatings are characterized by an adhesion higher than 70 MPa [78−80]. A perfect adhesion of EPT coatings seems to be determined by the formation of diffusion bonds with the substrate at the high local temperatures.

(iii) Grain structure of nanocrystallites, which determines the unique properties of nanostructured materials that are of primary interest for the science [73]. Nanocrystalline grains produced in the course of plasma-electrolytic treatment enable one to improve the characteristics of coatings compared to coarse-grain analogues.

Surface Composition and Structure

Structure investigations typically show the existence of three distinct sublayers in coatings obtained on aluminum alloys by plasma-electrolytic oxidation. A porous outer sublayer is composed chiefly of low-temperature X-ray amorphous phases. A compact inner sublayer is formed during the high-temperature modification; and complex phases composed of the substrate alloy elements constitute a thin interface layer below the compact one. Relative sizes of the sublayers, their structures, and compositions are substantially affected by the compositions of the substrate and electrolyte and conditions of treatment. Thorough investigation of the effects was carried out in the case of aluminum alloys treated in dissolved silicon. As was found, in alkaline solutions either individual or containing dissolved silicon (e.g., 2−20 g/L Na_2SiO_3 and 2−4 g/L KOH), the inner compact layer, which is composed chiefly of γ- and α-Al_2O_3 phases and contains also Al−Si−O complex phases, is broadened. The relative content of the more solid phase increases

with an increase in the current density. The content of α-aluminum can be as high as 60% in coatings formed on copper-containing aluminum substrates, while the γ-Al$_2$O$_3$ phase is predominantly formed on magnesium-containing aluminum alloys [80–83].

The increase in the concentration of silicate in the electrolyte results in the accelerated growth of the coating due to the inclusion of silicon in its structure and formation of Al–Si–O complex phases. In this way, an interlayer with a two-phase structure appears in which the phase ratio can vary in a broad range.

When silicon is present in an alkaline electrolyte, the distribution of elements in the thickness of the coating changes depending on the type of particles that contain silicon. For example, coatings formed in a 2-g/L alkaline solution containing no silicon are characterized by a homogeneous distribution of aluminum in the depth and the presence of special alloy additives, such as copper and magnesium, which are accumulated close to the outer surface according to the peculiarities of their interaction with oxygen.

The addition of sodium silicate in the amount of 15 g/L to the electrolyte results in penetration of 3–5 at % silicon in the coating and the substantial decrease in the concentration of copper and magnesium, which migrate to the interlayer. The location of the maximum content of copper and magnesium is also shifted toward the substrate. When silicon is introduced as a fine powder, its content in the coating increases (to 40–60% on the surface), but its distribution in the depth of the layer is no longer homogeneous. Accordingly, concentration profiles of aluminum and other alloy components also change. When alkaline solutions that contain dissolved silicon are used, the degree of uniformity of the thickness of the coating depends on the composition of the bath.

Homogeneous coatings can be obtained only in the presence of certain balanced combinations of silicon and alkali, and the increase in the concentration of silicate leads to stronger growth of the coating at the specimen edges where the polycondensation of silicon is facilitated due to the more intense sparking [84].

By contrast, an increase in the alkali concentration causes the local dissolution of the oxide layer and the formation of pits on the surface. Oxide coatings obtained in concentrated silicate solutions (50–300 g/L) are thicker and more homogeneous. However, their outer layers are also thicker and can constitute up to 90% of the whole thickness of the coating. Such layers are usually X-ray amorphous and contain 40–43% silicon, 1–4% aluminum, 1–4% sodium, and 49–58% oxygen. Silicate coatings typically have a foamlike structure with a high bulk porosity and relatively low mechanical properties. Composition of the coatings can be changed only by introducing additional substances to the electrolyte. For the purpose, electrolytes that contain Al$_2$O$_3$, Fe$_3$O$_4$, TiO$_2$, MgO, or Cr$_2$O$_3$ fine powders are often used. However, because of the high bulk porosity, the distribution of elements in the coatings is very heterogeneous.

Similarly to the usual treatment accompanied by thermal chemical diffusion, the surface layers produced on steels by plasma-electrolytic carbonitriding (PEN/C) involve two sublayers. The inner diffusion layer of pearlite and preserved austenite (that involves diffusion elements in solid solution) and the outer "white" layer primarily formed of iron nitrides and carbides have a diffuse interface. Characteristics of the structure zones depend on the voltage and conditions of treatment, as well as on the nature of the diffusing element.

Figure 7 shows SEM images of the cross sections of typical saturated surface layers obtained as a result of plasma electrolysis. A nitride coating usually involves an outer white layer bound to the inner diffusion layer, which contains a mixture of nitrides and nitrogen-containing carbides with a thickness of 40–50 μm (Fig. 7a). In a carbonitride coating, the boundary between the white layer and diffusion zone of α-Fe(C–N) carbonitride phases is more diffuse (Fig. 7b).

Probably because of the rapid cooling in an electrolyte flow, predominantly martensite structures are observed in the nitride coating. In the carbide coating, which was cooled in air (Fig. 7c), the white layer is thicker, while the diffusion zone, which is composed of cementite and pearlite, is thinner. The temperature of the process is very important, as it provides concurrent saturation with carbon and nitrogen.

Concentration profiles of nitrogen and carbon in the outer surface layer and inner diffusion layers formed either at 670 or 820°C were studied, and it was found that layers with a thickness of 100–150 μm or even up to 200 μm can be formed as early as in 3 min.

Nevertheless, the distribution of elements within the layer is not the same under different conditions. At 670°C, an outer white layer with a thickness of 10–20 μm that contains 5–6% N and only 0.7% C is formed, while the maximum content of carbon (1.23%) is typical of the inner layer at a depth of 100 μm. By contrast, at high temperatures, diffusion of carbon prevails over that of nitrogen. At 820°C, the process results in the decrease in the mean maximum content of nitrogen to 0.46% at a mean maximum content of carbon of 0.91%, which is now observed in the surface part. The microstructures of the outer and inner sublayers are as follows: the easily distinguishable outer (white) layer with a definite diffusion zone gradually transforms into a layer with an increased diffusion and composed chiefly of the high-quality carbon/nitrogen martensite.

Corrosion Behavior

Steels cleaned with EPT are resistant against general corrosion for a period of several days to several months in closed spaces (see e.g., Fig. 8) [84].
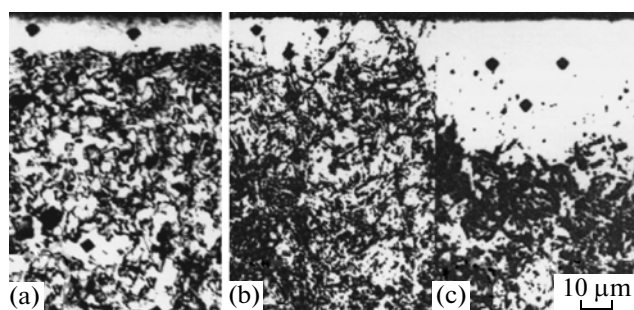
Fig. 7. Images of the cross section of a surface layer of 0.4C1.0Cr steel upon 4-min plasma-electrolytic (a) nitriding (PEN) at 640°C, (b) carbonitriding (PEN/C) at 800°C, and (c) oxidation (PEO) at 860°C.
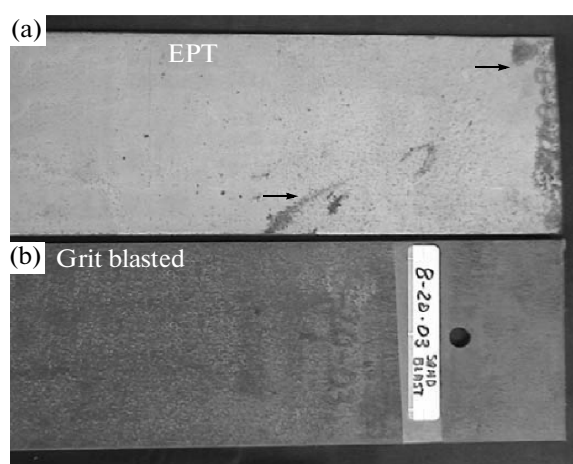

Fig. 8. Degree of corrosion destruction of a steel ribbon cleaned by (a) electrolytic plasma treatment and (b) grit blasting upon 6-month laboratory test at a relative humidity of 75% [15]. Arrows show regions of rust formation on EPT-cleaned specimen caused by accidental wet contact.

Electrochemical tests of specimens and measurements of such characteristics as the broken-circuit potential [73], linear polarization, and electrochemical resistance [84, 85] showed that the EPT-cleaned surfaces manifest high corrosion resistance. Investigation of the linear polarization showed [85] that the corrosion rate of the EPT-cleaned steel in 1 N H_2SO_4 and 3.5% NaCl is lower by an exponent compared to the steel upon grit blasting. This is due to the formation of an individual α-iron layer upon plasma-electrolytic cleaning [86−90].

Steel rods with a diameter of 5.5 μm cleaned by means of EPT were subjected to corrosion tests. Two weeks after cleaning, the rods were covered with copper and/or underwent tensile testing. No defect was discovered during elongation. It is well known that the presence of oxide or rust will cause exfoliation of copper from steel or breakage of the wire during a tensile test. The tests revealed the formation of passivated surface upon EPT cleaning in accord with the results of laboratory tests. The structure of nanoscale grains composed of individual α-iron formed on a EPT-cleaned steel surfaces can cause passivation. On nanocrystalline stainless steel 304, because of the fine grain structure, localized corrosion resistance was noted, in contrast to the usual stainless steel 304 [91, 92].

Friction Characteristics

Friction characteristics of oxide coatings under lubricated friction conditions were studied in oil and aqueous environments. The decrease in the coefficient of friction in an oxide−steel system from $\mu = 0.4$ typical of steel to $\mu \approx 0.015$ characteristic of the surface covered with a coating was noticed when the oxide film was impregnated with oil. Friction characteristics of the pin-on-disc system in the case of PEO coatings on aluminum alloys were determined in industrial and sea water. As was found, a combination of α-Al_2O_3 coatings is characterized by $\mu = 0.023−0.025$ at a pressure of up to 16 MPa. Two γ-Al_2O_3-based coatings had $\mu = 0.005−0.008$ up to a critical pressure of 8 MPa.

Two solids based on mullite coatings are characterized by a critical pressure of 4 MPa [92].

The coefficients of friction of the materials with complex mechanical properties, such as oxide coatings that contain Al_2O_3 or two types of coatings, depend chiefly on the tribochemical interactions between the surfaces brought in contact. The interactions strongly depend on the composition of the environment.

For example, an increase in air humidity to 80% provides the formation of a thin lubricating aluminum dioxide film, which results in the decrease in the coefficient of friction. Friction of materials with different mechanical properties, such as oxide coatings and steel or WC−Co, is accompanied by continuous reconstruction of the contact friction domain. As a result, chemical interaction in the contact domain between the needle accelerator and the surface leads to an increase in the coefficient of friction. In order to decrease the dry friction in the case of such solids, thin carbon films are plated on the surface of oxide coatings. This enables one to reach a coefficient of friction of 0.49−0.62 to 0.17−0.32 for the friction of reverse of a WC−Co ball. Recent studies have showed that the whole oxide coating can substantially affect the mechanical properties depending on the contact mode. Taking into account all tribological characteristics, thick PEO coatings exhibit better properties in the case of sliding friction, scratching, and colliding, whereas thin coatings are more effective in the case of collisions and easy sliding. PEO coatings of intermediate thickness have worst characteristics according to all tribological tests. There is a noticeable range within which the microstructure, composition, and thickness of the coatings can be varied to obtain optimum behavior under certain loading conditions. If the opti-

mum characteristics of aluminum PEO coatings with respect to loading are in question, there are numerous variants of developing new multilayer and hybrid-duplex coatings for aluminum protection [93–96].

Surface Doping

EPT has successfully been used for strengthening steels by surface doping, such as cementing [72], nitriding [92], carbonitriding [74], and boro-sulpho-carbonitriding. It is worth noting that the diffusion rate of different chemical compounds into metallic surfaces during electrolytic plasma processing is much higher than that at conventional procedures. For example, when Mo coating was plated on steel 4330V and Inconel 718 with the use of EPT [84], analysis of XRD data showed that Mo was built in the surface to produce an alloy rather than deposited as a coating. EPT-alloyed molybdenum made the coating twice as strong at different Mo contents [74]. Figure 9 shows the surface morphology (Fig. 9a, 9b) and surface profiles (Fig. 9c, 9d) upon scratching the surfaces of original and alloyed specimens. Although the coefficient of friction of the surface doped with molybdenum is slightly higher, the wearing intensity is lower by a factor of three compared to the original untreated surface (Figs. 9c, 9d). Thorough examination of the scratch traces shows that the mechanisms of wearing of the unprocessed steel and that doped with molybdenum differ (Figs. 9a, 9b).

Experiments, in which the surface of cast iron was strengthened, show that EPT enables one to strengthen the surface layer to a depth of 3 mm. The layer includes three zones with different structures. The subsurface layer has a fine-crystalline martensite structure and, hence, exhibits great microhardness. The value is nearly three times as high as that of the substrate material. Figure 10 shows the changes in the microhardness of the subsurface (strengthened) layer depending on the depth. As can be seen, the micro-hardness increases by a factor of 3 close to the surface. The maximum microhardness (7000 MPa) is observed at a depth of 1.2–2.5 mm. The total thickness of the strengthened layer is about 3 mm. Note that the dependence constructed has minimum and maximum points, which seem to be related to the formation of local domains of fine-crystalline martensite and coarse-grained substrate material.

Taking into account the fact that plasma-electrolytic treatment was carried out at repeatedly increased and decreased power density of heating, one can explain the corresponding periodicity in the changes of microhardness in the depth of the strengthened layer.

Concurrently with the layer-by-layer strengthening, the surface layer of cast iron can be alloyed also with the elements that are involved in the anode material, as well as with the elements contained or specially introduced in the electrolyte.
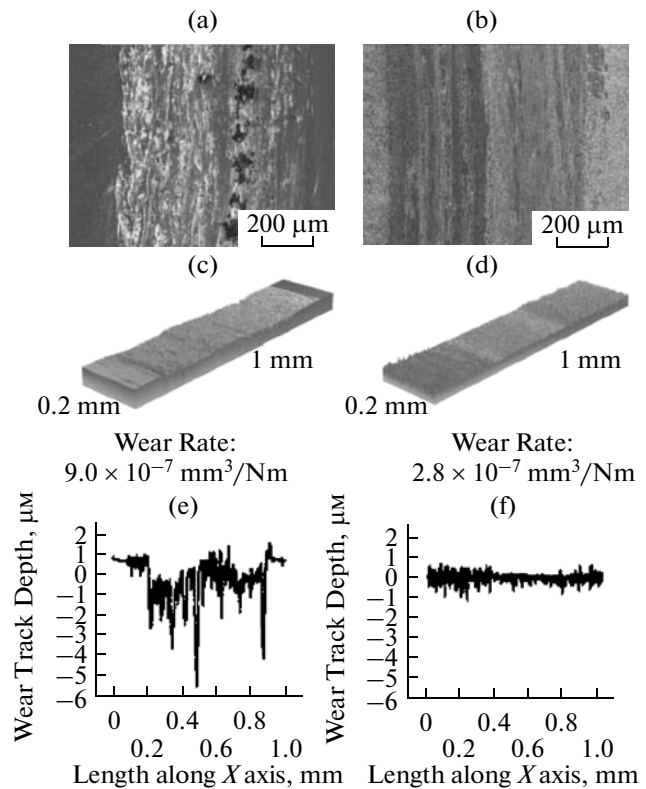

Fig. 9. Results of tribological test in pin-on-disc system for 440C steel: (a, c, e) original and (d, f) EPT-alloyed with Mo. (a, b) SEM images of scratch morphology, (c, d) 3D images of scratches, and (e, f) 2D images of scratches.

MODERN STATE OF EPT APPLICATIONS

Despite many years of investigations of the possibilities and applications of plasma-electrolytic treatment [93–99], transformation of the approach from a laboratory research technique into an industrial commercial method of metallurgy is not still a reality. Today, commercial applications are restricted to cleaning and coating wires, rods, and reinforcing bars (Fig. 11).

Practical applications of plasma electrolysis in recent years have showed that PEO coatings can successfully compete with those produced as a result of anodizing and thermal oxidation and are a real alternative to conventional composite materials in diverse branches of industry. Remarkable wear, friction, corrosion, and thermal resistance of the coatings is attractive for industrial production and promising in textile and aircraft industry, space engineering, gas extraction, petroleum production, and purification. Figure 12 shows a typical scheme of a device designed for local treatment of surface sites. For example, when strengthening of the outer surface of a drill rod or a planar sheet surface is required, a heating element has a cone shape (Figs. 12a, 12b), while the heated site spot is round or ellipsoidal. In order to increase the productivity, two to six heating elements can be simul-
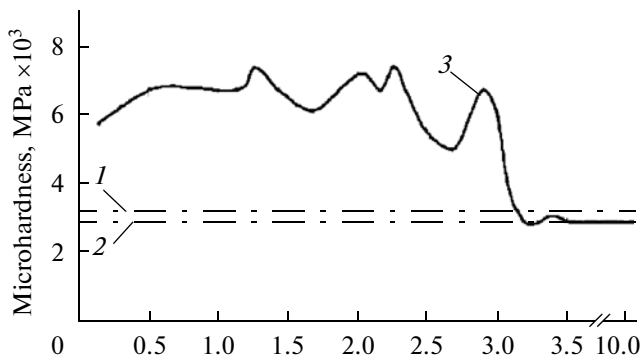
Fig. 10. Microhardness of cast iron specimen depending on the depth (cross section): (*1*) ferrite (original specimen), (*2*) pearlite (original specimen), and (*3*) specimen after PEO.

taneously used for the heat treatment. For strengthening aperture edges, special heating elements, in which the electrolyte is drained along the anode axis can be taken (Fig. 12b). The heating surface part is ring-shaped. Faces of items, e.g., bushes, can be quenched by immersing the part to be strengthened in an anode bowl filled with an electrolyte (Fig. 12c). In this case, thickness of the heated part of the item corresponds to the immersion depth in the bath [100].

Disc-shaped components, such as a circular saw, are strengthened with the use of an electrolytic heating element that is brought close to the bottom part of the component. Saw teeth or the peripheral part of the disc are immersed in the electrolyte and heated with the electric current passed. The inner surface of a cylinder can be strengthened with the use of a small-size heater that can be inserted in the component. Shifting the heating element along the inner axis of the cylinder enables one to form a strengthened layer, which can have different configurations. Arrangement of

strengthened sites depends on the trajectory of heating elements over the surface. The output nozzle of the heating element can have an arbitrary shape that will produce a specific desirable strengthened profile. Continuous motion of a heating element provides the formation of helical curves with different ascent angles on the surface. Strengthened sites typically have large sizes or resemble broad helix lines (15–50 mm in width), which provides the formation of a layer with inner compressive strains. The relatively low heating rate results in the formation of thick quenched layers with no general surface fritting.

Experience has shown that the plasma-electrolytic method is efficient in metallurgy, mining, and the agricultural industry [85–87], where certain local parts of items and components should be strengthened to a depth of 10 mm. Industrial tests of strengthened products, such as knives and saws for cutting metal, drill pipe lock joints, panlines of scraper production lines, tool posts of shaft-sinking sets, discs of harrows, crusher hammers, etc., showed that the strengthened products have a service and working capacity two or three times as high as that of those that were not strengthened.

The kind and composition of equipment for plasma-electrolytic treatment depend on the configuration and weight of items to be strengthened [96–101]. For example, the surface strengthening of cylindrical components such as axles or shafts can be carried out on a standard handler (lathe). The component is mounted in the center, and heating elements are mounted on the lathe casing. Electrolyte is supplied from a container that stands aside. The electric-energy transformer is one of those conventionally used in plasma techniques. Electrolytic heating elements and control desks on their own are nonstandard [101].
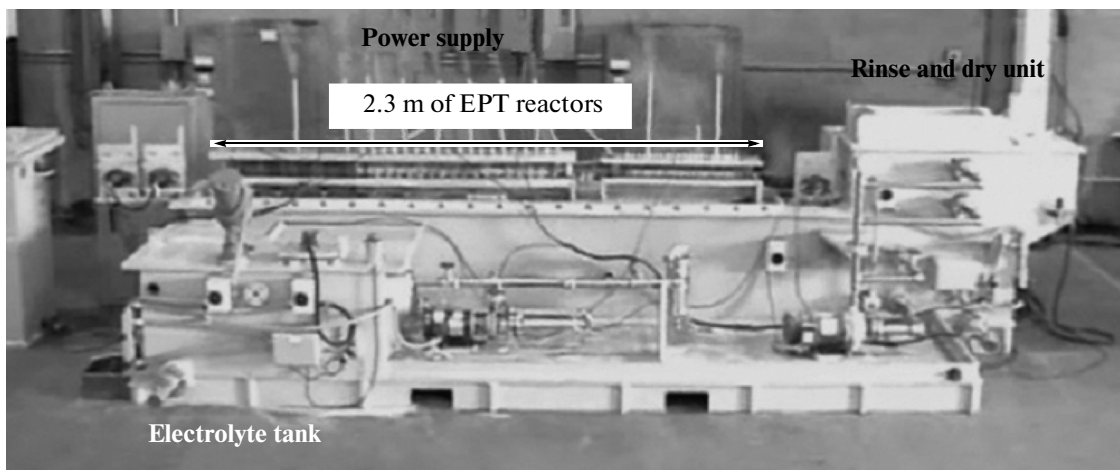

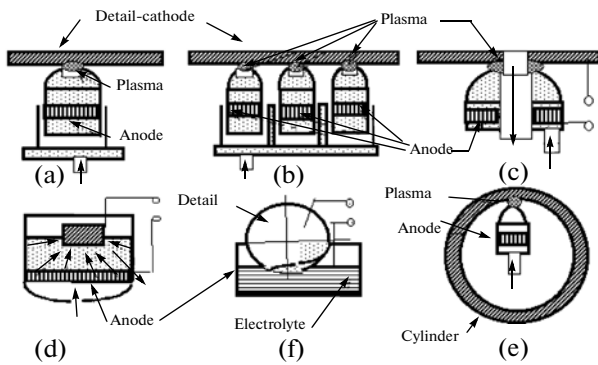**Fig. 11.** Industrial unit for electrolytic plasma processing of rods.

Fig. 12. Schemes of technological units for electrolytic plasma strengthening of detail parts: (a, b, c) planar surfaces, (d) face, (e) inner surface of a cylinder, and (f) peripheral part of a saw disc.

CONCLUSIONS

A review of the processes of electrochemical treatment that are classified as plasma electrolysis has been given. Special attention has been paid to the chemical and physical processes in an electrolyte, as well as to the technique of plating protective coatings and modifying surfaces. Results of the investigation of the coatings and surfaces upon plasma-electrolytic treatment, which show the efficiency and effectiveness of the method, are considered. Being an efficient method of surface treatment that combines surface cleaning and covering with a coating, plasma-electrolytic treatment has now been put into practice for commercial use.

REFERENCES

1. Sluginov, N.P., *Zh. Russ. Fiz.-Khim. Obshchestva*, 1878, vol. 10, no. 8, p. 241.
2. Gunterschultze, A. and Betz, H., *Electrolytkondensatoren*, Berlin: Krayn, 1937.
3. McNiell, W. and Nordbloom, G.F., US Patent 2854390, 1958.
4. McNiell, W. and Gross, L.L., US Patent 3293158, 1966.
5. Markov, G.V. and Markova, G.A., USSR Inventor's Certificate no. 526961, *Byull. Izobret.*, 1976, no. 32.
6. Nikolaev, A.V., Markov, G.A., and Peshchevitskii, B.N., *Izv. Sib. Otd. Akad. Nauk SSSR, Ser. Khim. Nauk*, 1977, no. 5, p. 32.
7. Markov, G.A., Terleeva, O.P., and Shulepko, E.K., *Izv. Sib. Otd. Akad. Nauk SSSR, Ser. Khim. Nauk*, 1983, vol. 7, no. 3, p. 31.
8. Gordienko, P.S., *Obrazovanie pokrytii na anodnopolyarizovannykh elektrodakh v vodnykh elektrolitakh pri potentsialakh proboya i iskreniya* (Formation of Coatings on Anodically Polarized Electrodes in Aqueous Electrolytes at Breakdown and Sparking Potentials), Vladivostok: Dal'nauka, 1996.
9. Gordienko, P.S. and Gnedenkov, S.V., *Mikrodugovoe oksidirovanie titana i ego splavov* (Micro-Arc Oxidation of Titanium and Its Alloys), Vladivostok: Dal'nauka, 1997.
10. Malyshev, V.N., Markov, G.A., Fedorov, V.A., et al., *Khim. Neftyanoe Mashinostroenie,* 1984, no. 1, p. 26.
11. Kurze, P., Krysmann, W., Marx, G., and Wiss, Z., *Tech. Hochsch. Karl-Marx-Stadt*, 1982, vol. 24, p. 139.
12. Dittrich, K.H., Krysmann, W., Kurze, P., and Schneider, H.G., *Cryst. Res. Technol.*, 1984, vol. 19, p. 93.
13. Krysmann, W., Kurze, P., Dittrich, K.H., and Schneider, H.G., *Cryst. Res. Technol.*, 1984, vol. 19, p. 973.
14. Markov, G.A., Shulepko, E.K., and Zhukov, M.F., USSR Inventor's Certificate no. 926084, *Byull. Izobret.*, 1982, no. 17.
15. Karanik, Yu.A., Markov, G.A., Minin, V.F., et al., USSR Inventor's Certificate no. 582894, *Byul. Izobret.*, 1977, no. 45.
16. Brown, S.D., Kuna, K.J., and Van, T.B., *J. Am. Ceram. Soc.*, 1971, vol. 54, p. 384.
17. Van, T.B., Brown, S.D., and Wirtz, G.P., *Am. Ceram. Soc. Bull.*, 1977, vol. 56, p. 563.
18. Yerokhin, A.L., Snizhko, L.O., Gurevina, N.L., et al., *J. Phys. D: Appl. Phys.*, 2003, vol. 36, p. 2110.
19. Huang, P., Wang, F., Kewei, X., and Han, Y., *J. Surf. Coat. Technol.*, 2007, vol. 201, p. 5168.
20. Ceschini, L., Lanzoni, E., Martini, C., et al., *Wear*, 2008, vol. 264, p. 86.
21. Markov, G.A., Tatarchuk, V.V., and Mironova, M.K., *Izv. Sib. Otd. Akad. Nauk SSSR, Ser. Khim. Nauk*, 1983, vol. 7, no. 2, p. 34.
22. Wei, C.B., Tian, X.B., Yang, S.Q., et al., *Surf. Coat. Technol.*, 2007, vol. 201, p. 5021.
23. Habazaki, H., Onodera, T., Fushimi, K., et al., *Surf. Coat. Technol.*, 2007, vol. 201, p. 8730.
24. Titorenko, O.V., Rat'kova, E.A., and Savel'eva, E.A., Abstracts of Papers, *Sovremennye Elektrokhimicheskie Tekhnologii. Nauchno Tekhnicheskaya Konferentsiya* (Modern Electrochemical Techniques. Technical Scientific Conf.), Saratov, 1996, p. 51.
25. Petrosyants, A.A., Malyshev, V.N., Fedorov, V.A., and Markov, G.A., *Trenie Iznos*, 1984, vol. 5, no. 2, p. 350.
26. Voevodin, A.A., Yerokhin, A.L., Lyubimov, V.V., et al., *Surf. Coat. Technol.*, 1996, vols. 86−87, p. 516.
27. Yerokhin, A.L., Voevodin, A.A., Lyubimov, V.V., et al., *Surf. Coat. Technol.*, 1998, vol. 110, p. 140.
28. Saakyan, L.S., Efremov, A.P., and Soboleva, I.A., *Zashch. Met.*, 1994, vol. 30, p. 101.
29. Gnedenkov, S.V., Krisanfova, O.A., Zavidnaya, A.G., et al., *Prot. Met.*, 1999, vol. 35, no. 5, p. 480.
30. Sundararajan, G. and Krishna, L.R., *Surf. Coat. Technol.*, 2003, vol. 167, p. 269.
31. Wei, T., Yan, F., and Tian, J., *J. Alloys Compd.*, 2005, vol. 389, nos. 1−2, p. 169.
32. Yerokhin, A.L., Lyubimov, V.V., and Ashitkov, R.V., *Ceram. Int.*, 1998, vol. 24, p. 1.
33. Guangliang, Y., Xianyi, L., Yizhen, B., et al., *J. Alloys Compd.*, 2002, vol. 345, nos. 1−2, p. 196.
34. Xin, S.G., Jiang, Z.H., Wang, F.P., et al., *J. Mater. Sci. Technol.*, 2001, vol. 17, no. 6, p. 657.

35. Wu, H.H., Wang, J.B., Long, B.Y., et al., *Acta Phys. Sin.*, 2005, vol. 54, no. 12, p. 5743.

36. Wang, K., Koo, B.-H., Lee, C.-G., et al., *Trans. Nonferrous Met. Soc. China*, 2009, vol. 19, no. 4, p. 866.

37. He, G. and Hagiwara, M., *J. Mater. Sci. Eng.*, 2006, vol. 26, p. 14.

38. Guo, H.F. and An, M.Z., *Appl. Surf. Sci.*, 2005, vol. 246, p. 229.

39. Zozulin, A.J. and Bartak, D.E., *Met. Finish.*, 1994, vol. 92, p. 39.

40. Sharma, A.K., Uma, R.R., Malek, A., et al., *Met. Finish.*, 1996, vol. 94, p. 16.

41. Gupta, P., Tenhundfeld, G., Daigle, E.O., and Schilling, P.J., *Surf. Coat. Technol.*, 2005, vol. 200, p. 1587.

42. Wang, Y., Lei, T., Jiang, B., and Guo, L., *Appl. Surf. Sci.*, 2004, vol. 233, p. 258.

43. Ko, Y.G., Namgung, S., and Shin, D.H., *Surf. Coat. Technol.*, 2010, vol. 205, p. 2525.

44. Kim, Y.M., Hwang, D.Y., Lee, C.W., et al., *J. Met. Mater.*, 2010, vol. 48, p. 49.

45. Li, H.X., Rudnev, V.S., Zheng, X.H., et al., *J. Alloys Compd.*, 2008, vol. 462, p. 99.

46. Duan, H.P., Yan, C.W., and Wang, F.H., *Electrochim. Acta*, 2007, vol. 52, p. 5002.

47. Gu, W.C., Lv, G.H., Chen, H., et al., *J. Alloys Compd.*, 2007, vol. 430, p. 308.

48. Snizhko, L.O., Yerokhin, A.L., Pilkington, A., et al., *Electrochim. Acta*, 2004, vol. 49, p. 2085.

49. Xu, J.L., Liu, F., and Wang, F.P., et al., *J. Alloys Compd.*, 2009, vol. 472, p. 276.

50. Liang, J., Guo, B.G., Tian, J., et al., *Appl. Surf. Sci.*, 2005, vol. 252, p. 345.

51. Chang, L., *J. Alloys Compd.*, 2009, vol. 468, p. 462.

52. Cai, Q.Z., Wang, L.S., Wei, B.K., et al., *Surf. Coat. Technol.*, 2006, vol. 200, p. 3727.

53. Duan, H.P., Du, K.Q., Yan, C.W., and Wang, F.H., *Electrochim. Acta*, 2006, vol. 51, p. 2898.

54. Ko, Y.G., Lee, K.M., Shin, K.R., and Shin, D.H., *Kor. J. Met. Mater.*, 2010, vol. 48, p. 724.

55. Kharitonov, V.V., Plaskeev, A.A., Fedoseev, V.N., and Voskoboinikov, V.V., *High Temp.*, 1988, vol. 25, p. 700.

56. Mazza, B., Pedeferri, P., and Re, G., *Electrochim. Acta*, 1978, vol. 23, p. 87.

57. Usmani, S. and Sampath, S., *Wear*, 1999, vols. 225–229, p. 1131.

58. Meletis, E.I., Nie, X., Wang, F., and Jiang, J.C., *Surf. Coat. Technol.*, 2002, vol. 150, p. 246.

59. Gupta, P., Tenhundfeld, G., and Daigle, E.O., *Wire J. Int.*, 2005, vol. 38, p. 50.

60. Gupta, P. and Tenhundfeld, G., *Plat. Surf. Finish.*, 1005, vol. 92, p. 48.

61. Tjong, S.C. and Cheng, H., *Mater. Sci. Eng., R*, 2004, vol. 45, p. 1.

62. Lonyuk, B., Apachite, I., and Duszczyk, J., *Surf. Coat. Technol.*, 2007, vol. 201, p. 8688.

63. Badawi, F. and Villain, P., *J. Appl. Crystallogr.*, 2003, vol. 36, nos. 3–2, p. 869.

64. Fitzpatrick, M.E., Fry, A.T., Holdway, P., et al., *Determination of Residual Stresses by X-ray Diffraction. Measurement Good Practice Guide, no. 52. NPL*, Teddington: Middlesex, 2002.

65. Noyan, I.C. and Cohen, J.B., *Residual Stress Measurement by Diffraction and Interpretation*, New York: Springer, 1987.

66. Chernenko, V.I., Snezhko, L.A., and Papanova, I.I., *Poluchenie pokrytii anodno-iskrovym elektrolizom* (Plating Coatings by Anodic Sparking Electrolysis), Leningrad: Khimiya, 1991.

67. Pogrebnyak, A.D., Tyurin, Yu.N., Boiko, A.G., et al., *Usp. Fiz. Metallov*, 2005, vol. 6, p. 273.

68. Gordienko, P.S., *Obrazovanie pokrytii na anodno polyarizovannykh elektrodakh v vodnykh elektrolitakh pri potentsialakh iskreniya i proboya* (Formation of Coatings on Anodically Polarized Electrodes in Aqueous Electrolytes at Sparking and Breakdown Potentials), Vladivostok: Dal'nauka, 1996.

69. Atroshchenko, E.S., Kazantsev, I.A., and Rozen, A.E., *Novye promyshlennye tekhnologii. Tekhnicheskii progress v atomnoi promyshlennosti. Seriya — Tekhnologiya montazhnykh rabot*, (New Industrial Techniques. Technological Advances in Nuclear Power Industry. Technology of Installation Work), Moscow, 1996, no. 1.

70. Markov, G.A., Gizatullin, B.S., and Rychazhkova, I.E., USSR Inventor's Certificate no. 926083, *Byull. Izobret.*, 1982, no. 17.

71. Pogrebnjak, A.D., Kul'ment'eva, O.P., Kobzev, A.P., et al., *Tech. Phys. Lett.*, 2003, vol. 29, p. 312.

72. Nie, X., Hao, Q., and Wei, J., *Wuhan Univ. Technol.*, 1996, vol. 11, p. 28.

73. Gupta, P., Tenhundfeld, G., Daigle, E.O., and Schilling, P.J., *Surf. Coat. Technol.*, 2005, vol. 200, p. 1587.

74. Wayne, S.F., Sampath, S., and Anand, V., *Trib. Trans.*, 1994, vol. 373, p. 636.

75. Pogrebnjak, A.D., Lozovan, A.A., Kirik, G.V., et al., *Struktura i svoistva nanokompozitnykh, gibridnykh i polimernykh pokrytii* (Structure and Properties of Nanocomposite, Hybrid, and Polymer Coatings), Moscow: URSS, 2011.

76. Tyurin, Yu.N. and Pogrebnjak, A.D., *Surf. Coat. Technol.*, 2001, vols. 142–144, p. 293.

77. Gorelik, S.S., Rastorguev, L.N., and Skakov, Yu.A., *Rentgenograficheskii i elektronnoopticheskii analiz* (X-Ray Diffraction and Electron-Optical Analysis), Moscow: Metallurgiya, 1970.

78. Bar'yakhtar, V.G., Buravlev, Yu.M., Shevchenko, V.P., et al., *Trudy mezhdunarodnoi konerentsii "Oborudovanie i tekhnologii termicheskoi obrabotki metallov i splavov v mashinostroenii* (Proc. Int. Conf. "Equipment and Technologies in Thermal Treatment of Metals and Alloys in Engineering Industry"), Kharkiv: NNTs KhFTI, 2000, p. 155.

79. Tyulyapin, A.I., Tyurin, Yu.N., and Trainov, A.I., *Metalloved. Term. Obrab. Met.*, 1998, vol. 1, p. 9.

80. Eretnev, K.N. and Lebedev, S.V., *Protsessy nagreva i ochistki poverkhnosti metallov v elektrolite i ikh prakticheskoe ispol'zovanie* (Processes of Heating and Cleaning of Metal Surfaces in Electrolytes and Their Practical Application), Leningrad, 1997.

81. Kolachev, B.A., Elagin, V.I., and Livanov, V.A., *Metallovedenie i termicheskaya obrabotka tsvetnykh metallov i splavov* (Metal Research and Thermal Treatment of Non-Ferrous Metals and Alloys), Moscow: MISIS, 2001.

82. *Svoistva elementov: spravochnik* (Properties of Elements: Handbook), Drits, M.E., Ed., Moscow: Metallurgiya, 1997.

83. Luchikov, L.P., *Deformiruemye alyuminievye splavy dlya raboty pri povyshennykh temperaturakh* (Wrought Aluminum Alloys for Operation at Heightened Temperatures), Moscow: Metallurgiya, 1965.

84. Tyurin, Yu.N. and Pogrebnyak, A.D., *Tech. Phys.,* 2002, no. 11, p. 1463.

85. USSR Inventor's Certificate no. 1488321, *Byull. Izobret.*, 1987, no. 33.

86. USSR Inventor's Certificate no. 2138564, *Byull. Izobret.*, 1999, no. 27.

87. USSR Inventor's Certificate no. 1546362, *Byull. Izobret.*, 1988, no. 16.

88. Kulikov, I.S., Vashchenko, S.V., and Kamenev, A.Ya., *Elektrolitno-plazmennaya obrabotka materialov* (Electrolytic Plasma Processing of Materials), Minsk: Belaruskaya navuka, 2010.

89. Kadyrzhanov, K.K., Komarov, F.F., Pogrebnyak, A.D., et al., *Ionno-plazmennaya i ionno-luchevaya obrabotka materialov* (Plasma Ion and Ion Beam Processing of Materials), Moscow: MGU, 2005.

90. Parfenov, E.V., Yerokhin, A.L., and Matthews, A., *Surf. Coat. Technol.*, 2007, vol. 201, p. 8661.

91. Gupta, P., Tenhundfeld, G., Daigle, E.O., et al., *Surf. Coat. Technol.*, 2007, vol. 201, p. 8746.

92. Pogrebnyak, A.D., Kylyshkanov, M.K., Tyurin, Yu.N., et al., *Tech. Phys.*, 2012, vol. 57, no. 6, p. 840.

93. Zhukov, M.F., Dandaron, G.B., Zambalaev, Zh.Zh., and Fedotov, V.A., *Izv. Sib. Otd. Akad. Nauk SSSR, Ser. Tekhn. Nauk*, 1984, vol. 4, p. 100.

94. Pogrebnyak, A.D., Kylyshkanov, M.K., Bratushka, S.N., et al., *Phys. Surf. Eng.*, 2008, vol. 6, p. 73.

95. Pogrebnjak, A.D. and Beresnev, V.M., *Nanocoatings Nanosystems Nanotechnology*, New-York: Bentham Science, 2012.

96. Azarenkov, N.A., Beresnev, V.M., Pogrebnyak, A.D., et al., *Nanomaterialy, Nanopokrytiya, nanotekhnologii* (Nanomaterials, Nanocoatings, Nanotechnology), Kharkiv: KhNU, 2009.

97. P. Misaelides, A. Hatzidimitriou, F. Noli, A.D. Pogrebnjak et. al. *Surf. and Coat. Technol.*, 2004, vols. 180−181, p. 290-296.

98. Yerokhin, A.L., Nie, X., Leyland, A., et al., *Surf. Coat. Technol.*, 1999, vol. 122, p. 73.

99. Pogrebnjak, A.D., Dyadyura, K.A., Kylyshkanov, M.K., et al., *Kompressor. Energetich. Mashinostroenie*, 2005, vol. 4, no. 6, p. 105.

100. Pogrebnjak, A.D., Gritsenko, B.P., Kylyshkanov, M.K., et al., *Tech. Phys. Lett.*, 2006, vol. 32, no. 12, p. 1060.

101. Kylyshkanov, M.K., Kolebaev, K.K., and Pogrebnjak, A.D., Kazakhstan Patent no. S21D78, 2009.

Translated by Y.V. Novakovskaya